

Spinodal temperatures for macroscopic density fluctuations in Pd-H. II. Elastic constants above the critical point

This article has been downloaded from IOPscience. Please scroll down to see the full text article.

1992 J. Phys.: Condens. Matter 4 2149

(<http://iopscience.iop.org/0953-8984/4/9/009>)

View [the table of contents for this issue](#), or go to the [journal homepage](#) for more

Download details:

IP Address: 171.66.16.159

The article was downloaded on 12/05/2010 at 11:24

Please note that [terms and conditions apply](#).

Spinodal temperatures for macroscopic density fluctuations in Pd–H: II. Elastic constants above the critical point

M Sandys-Wunsch and F D Manchester

Department of Physics, University of Toronto, Toronto, Ontario, Canada M5S 1A7

Received 22 April 1991, in final form 22 October 1991

Abstract. Ultrasonic velocity measurements were made on Pd–H in the pressure and temperature regime above the critical point of the $\alpha \rightarrow \beta$ transition. The results were used to determine the elastic constants for the system and to compute the spinodal temperatures for the macroscopic density fluctuations near the critical point.

1. Introduction

The theory of Wagner and Horner [1–3] on the behaviour of metal hydrogen systems has determined that the dominant interaction among interstitial hydrogens in the region of the critical point is the elastic interaction mediated by the underlying metal lattice. Thus it is necessary to measure the parameters of the elastic interaction, in this region of the phase diagram, in order to fully describe the behaviour of the metal–hydrogen system.

In the previous paper, I, the determination of the characteristic energies for the macroscopic hydrogen density modes in terms of the measured elastic constants of the metal–hydrogen lattice was treated. We discuss here the experimental measurement of the elastic constants of the Pd–H system, and apply the results to the thin Pd–H disc analysed in I.

1.1. The experimental apparatus

The *in situ* apparatus allowed the ambient hydrogen pressure and temperature to be continuously varied, and the isotherm data of de Ribaupierre and Manchester [4, 5] and Wicke and Blaurock [6] were used to determine the hydrogen content of the sample. A Matec model 560 RF pulse generator (Matec Inc, Providence, Rhode Island, USA) produced pulses of 15 MHz sound, and an oscilloscope was used to track the reflection signals. The time elapsed between successive reflection peaks, together with the length of the sample, determined the sound velocity and hence the elastic constants [7].

The samples were single-crystal palladium supplied by Metals Research Ltd, UK, and were oriented to within a half degree along the [111] and [110] axes using the Laué back-reflection method. After spark-cutting into shape, the ends were finished with diamond paste to within 2 μm parallelism. The surface was carefully degreased and

etched before commencing the bonding procedure used to affix a quartz crystal transducer.

1.2. Transducer bonding

Quartz crystal transducers (Valpey-Fisher Co., Hopkinton, Massachusetts, USA) were attached to the palladium crystals with polyimide die adhesive (Transene Co., Rowley, New Hampshire, USA). This adhesive polymerizes at 270 °C and was found to be resilient to the large strains which result from loading the sample with hydrogen to the critical concentration. Several attempts were usually necessary to obtain a working bond that would tolerate hydrogen-loading of the sample. The mismatch in expansion between the palladium crystal and the transducer, $\Delta l/l_0 \approx 1\%$ at the critical point, limited the regime in which reliable measurements could be made to a hydrogen concentration of no more than $H/Pd = 0.4$.

2. Results

The velocity varied linearly with changing concentration and pressure. In contrast to the low-temperature behaviour [8, 9] the variation with temperature was small and did not depend significantly on the hydrogen concentration. The relative change in velocity is plotted in figure 1, with the temperature variation corrected, for longitudinal propagation along a [110] direction. The linear expansion of the palladium sample heated through a temperature change ΔT and loaded to hydrogen concentration ρ is [4]

$$\Delta l/l_0 = 0.066\rho + (1.15 + 6.3\rho) \times 10^{-5} \Delta T \quad (2.1)$$

The elastic constants are directly related to the velocities as shown in, for example, Bhatia [7]. Four combinations of elastic constants were determined. The longitudinal propagation along [110] is given by

$$v_l = \sqrt{(C_{11} + C_{12} + 2C_{44})/2d} \quad (2.2)$$

where d is the density of the metal-hydrogen sample. The transverse velocity excited in the [001] direction is

$$v_t = \sqrt{C_{44}/d}. \quad (2.3)$$

Longitudinal propagation along [111] has velocity

$$v_l = \sqrt{(C_{11} + 2C_{12} + 4C_{44})/3d} \quad (2.4)$$

and the transverse velocity

$$v_t = \sqrt{(C_{11} - C_{12} + C_{44})/3d}. \quad (2.5)$$

Corrections must be made to allow for the expansion of the palladium lattice and the adiabatic nature of the constants measured. This latter correction [7] to obtain the isothermal constants C^T from the set of adiabatic constants, C^S , is

$$C_{11}^T - C_{11}^S = C_{12}^T - C_{12}^S \approx -(T/C_V)(C_{11}^S + 2C_{12}^S)^2 \alpha^2 \quad (2.6)$$

$$C_{44}^T - C_{44}^S = 0 \quad (2.7)$$

where α is the coefficient of linear thermal expansion. This is a correction of only about

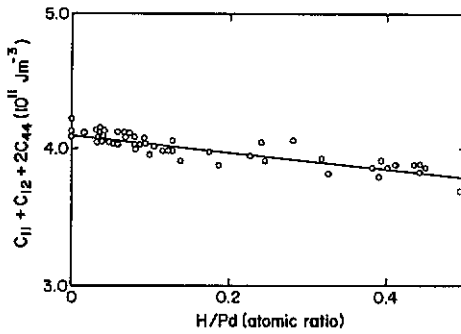


Figure 1. $C_{11} + C_{12} + 2C_{44}$, corrected for temperature variations, versus hydrogen density.

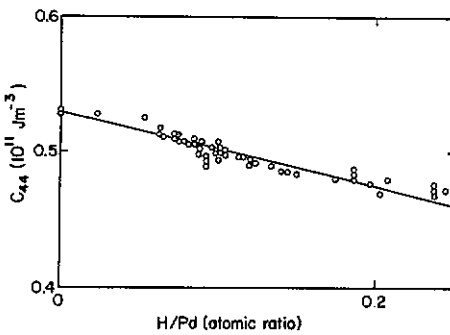


Figure 2. C_{44} , corrected for temperature variations, versus hydrogen density.

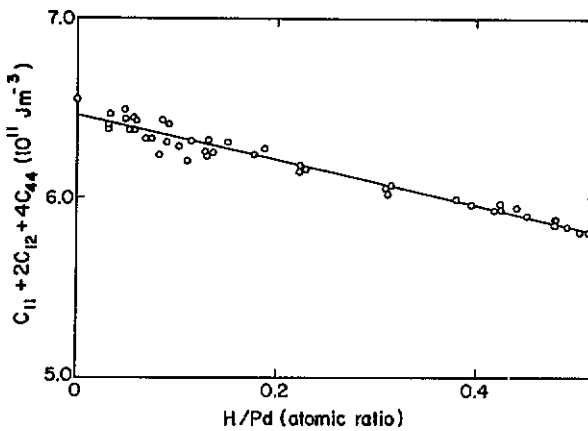


Figure 3. $C_{11} + 2C_{12} + 4C_{44}$, corrected for temperature variations, versus hydrogen density.

1% at the critical point. The four combinations of elastic constants, which are related to velocities of propagation (equations (2.2-2.5)) are plotted as functions of the hydrogen density in figures 1-4, respectively, with a straight-line regression fit. Regression fits for the elastic constants are shown in table 1. For comparison, previous work at lower

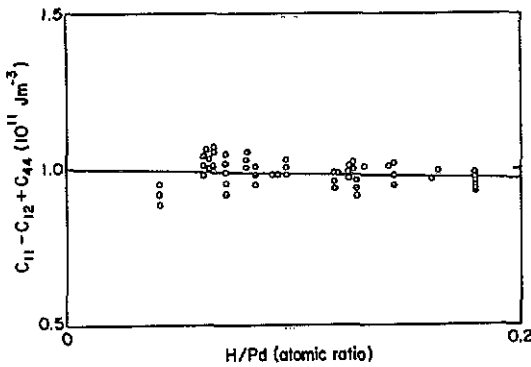


Figure 4. $C_{11} - C_{12} + C_{44}$, corrected for temperature variations, versus hydrogen density.

Table 1. Isothermal elastic constants in 10^{11} J m^{-3} . Data from Geerken *et al* [8] and Hsu and Leisure [9], values at 300 K (upper part of table) and from the present work, temperature 300–350 °C, ρ between 0 and 0.40 (lower part of table).

	Pd	PdH _{0.66}
C_{11}	2.2378	2.1088
C_{12}	1.7312	1.5665
C_{44}	0.7125	0.6345
C_{11}	$1.736 - 8.2 \times 10^{-4} \text{ K}^{-1}(T - 566) - 0.11\rho$	
C_{12}	$1.19 + 7.9 \times 10^{-4} \text{ K}^{-1}(T - 566) + 0.11\rho$	
C_{44}	$0.576 - 5.4 \times 10^{-4} \text{ K}^{-1}(T - 566) - 0.37\rho$	

temperatures is also shown. Note that the hydrogen density is expressed as the (dimensionless) ratio H/Pd.

3. Discussion

The eigenenergies for macroscopic modes involve the elastic constants evaluated at the particular temperature and pressure point being considered for a mode. A problem arises with choosing the appropriate set of constants to use, for the phenomena of long-range fluctuations occur only in coherent metal–hydrogen crystals, where the full set of cubic constants is appropriate, while the theory applies to isotropic systems, with the exception of the weakly anisotropic sphere [10]. Further, measurement of the proper cubic constants is not really possible below the incoherent spinodal, for then the system undergoes plastic deformation and becomes polycrystalline.

The discussion of isotropy is a little ambiguous, but one may follow Mason [11] and define effective isotropic constants for the case where the system becomes completely polycrystalline. Then the Lamé constants are

$$\lambda = C_{11} - 2C_{44} - \frac{1}{3}q \quad \mu = C_{44} + \frac{1}{3}q \quad (3.1)$$

where

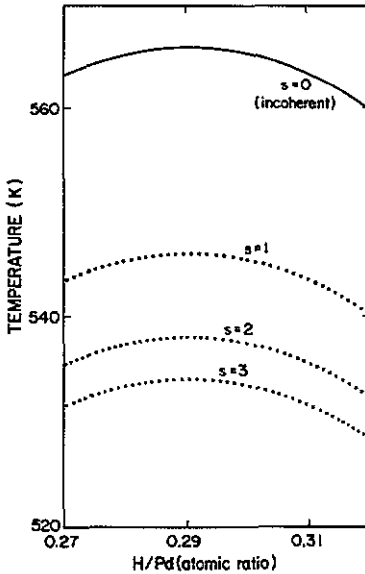


Figure 5. Spinodal curves for the first four macroscopic density modes. The complexity of the dilation is measured by the number s , which describes the highest power of r in the expression for the dilation. Each of the spinodal curves represents a family of (almost degenerate) modes, differing only in the angular variation, as characterized by the integer l .

$$q \equiv C_{11} - C_{12} - 2C_{44}. \tag{3.2}$$

Thus the Lamé constants at the critical point may be taken as

$$\lambda \approx 1.136 \pm 0.008 \times 10^{11} \text{ J m}^{-3} \tag{3.3}$$

$$\mu \approx 0.377 \pm 0.005 \times 10^{11} \text{ J m}^{-3}. \tag{3.4}$$

Wagner and Horner [1] have shown that, near the critical point, only the first few macroscopic modes would contribute much to the critical behaviour. Considering a disc as treated in I, and using a circular polar coordinate system aligned with the disc sample, the first three modes are

$$\Phi_{1,0} \equiv [V(R^4/48 + 4L^4/45)]^{-1/2} [(z^2 - \frac{1}{2}r^2) + (\frac{1}{3}R^2 - \frac{1}{3}L^2)] \tag{3.5}$$

$$\Psi_{0,0} = [V/3]^{-1/2} z \tag{3.6}$$

$$\Psi_{1,0} = [V(L^2R^4/16 + 4L^6/175)]^{-1/2} [(z^3 - \frac{3}{2}zr^2) + (\frac{3}{8}LR^2 - \frac{3}{8}L^3)]. \tag{3.7}$$

The constant gradient mode, $\Psi_{0,0}$, is degenerate with the (incoherent) constant density mode, but the other two are suppressed by an amount

$$\Delta_l \equiv T_c - T_l \approx 20 \text{ K}. \tag{3.8}$$

This follows from using the formulae for the spinodal apex temperatures from I

$$T_{s,l} = \omega_{s,l}/k_B f_2 \tag{3.9}$$

where $\omega_{s,l}$ is the eigenvalue for the mode described by numbers s and l ,

$$\omega_{s,l} \approx 3.3 \text{ eV}^2 / \left[\lambda + \mu \left(\frac{2s+2}{2s+3} + \frac{l(l-1)}{(s+1)(2s+3)^2} \frac{L^2}{R^2} + \dots \right) \right] \tag{3.10}$$

for odd parity modes, k_B is Boltzmann's constant, and f_2 is the second derivative of the

reference free-energy density, evaluated for a constant density distribution. Substituting in the values (3.3) and (3.4) for the elastic constants,

$$T_{s,l} \approx 691 / \left[1 + 0.332 \left(\frac{2s+2}{2s+3} + \dots \right) \right]. \quad (3.11)$$

The spinodal curves are shown near the critical density for the first few macroscopic modes in figure 5.

4. Conclusions

The elastic constants of the palladium–hydrogen system were found to vary regularly near the critical point, an indication that while the hydrogen interstitials are undergoing a phase transition, the underlying palladium lattice is basically unaffected by the presence of a critical point. This supports the concept of the system as a good example of a lattice gas, as put forward by Hill [12]. The separation of the spinodal temperatures for the modes in a thin disc should be accessible experimentally.

Acknowledgments

This work was supported by the Natural Sciences and Engineering Research Council of Canada, and by the University of Toronto, through a J C McLennan scholarship to M Sandys-Wunsch.

References

- [1] Wagner H and Horner H 1974 *Adv. Phys.* **23** 587
- [2] Bausch R, Horner H and Wagner H 1975 *J. Phys. C: Solid State Phys.* **8** 2559
- [3] Horner H and Wagner H 1974 *J. Phys. C: Solid State Phys.* **7** 3305
- [4] de Ribaupierre Y and Manchester F D 1974 *J. Phys. C: Solid State Phys.* **7** 2126
- [5] de Ribaupierre Y and Manchester F D 1975 *J. Phys. C: Solid State Phys.* **8** 1339
- [6] Wicke E and Blaurock J 1987 *J. Less-Common Met.* **130** 351
- [7] Bhatia A B 1967 *Ultrasonic Absorption* (Oxford: Oxford University Press) ch 3
- [8] Geerken B M, Griessen R, Huisman L M and Walker E 1982 *Phys. Rev. B* **26** 1637
- [9] Hsu D K and Leisure R G 1979 *Phys. Rev. B* **20** 1339
- [10] Hirsekorn P and Siems R 1981 *Z. Phys. B* **40** 311
- [11] Mason W P 1950 *Piezoelectric Crystals and their Application to Ultrasonics* (New York: van Nostrand) ch 15
- [12] Hill T L 1960 *Introduction to Statistical Thermodynamics* (New York: Addison-Wesley) ch 14